Inelastic electron-magnon interaction and spin transfer torque

T. Balashov,[1] A. F. Takács,[1] M. Däne,[2] A. Ernst,[2] P. Bruno,[2,3] and W. Wulfhekel[1]

[1]*Physikalisches Institut, Universität Karlsruhe (TH), Wolfgang-Gaede Strasse 1, 76131 Karlsruhe, Germany*
[2]*Max-Planck-Institut für Mikrostrukturphysik, Weinberg 2, 06120 Halle, Germany*
[3]*European Synchrotron Radiation Facility, BP 220, F-38043 Grenoble Cedex, France*

A combined experimental and theoretical study on the inelastic transfer of spin momentum between a spin-polarized tunneling current and a ferromagnetic electrode is presented. Using inelastic tunneling spectroscopy across a vacuum gap at 4 K we show that high-energy magnons are efficiently excited in inelastic-scattering events and that the asymmetry of magnon excitation for tunneling into and out of the ferromagnet is proportional to the spin polarization of the tunneling current. We discuss the size of the resulting spin torque and explain the energy distribution of the excited magnons on basis of spin scattering mediated by the itinerant exchange interaction.

I. INTRODUCTION

The spin transfer torque (STT), in which the spins of the electrons in an electric current exert a torque on the magnetization of a magnetic electrode, is an effect of high fundamental interest[1,2] and large potential in applications.[3–5] According to the standard description of this effect derived by Slonczewski, the torque in all metal junctions is created by elastic electron scattering.[1] Following the observation of the STT in magnetic tunnel junctions[5–11] the additional parameter of bias voltage across the junction had to be considered. Inelastic contributions to the STT are currently discussed in both theory and experiments.[10,12,13] In sharp contrast to the importance of inelastic contributions to the STT, neither the size of the inelastic transfer of momentum between the current and the magnetization nor the energy spectrum of the excited magnons is known.

In this combined experimental and theoretical paper we observe magnon creation by inelastic scattering of electrons, relate the inelastic-scattering probability to the spin polarization of the tunneling current, explain the energy distribution of the created magnons on basis of electron-electron spin scattering and give quantitative values for contribution of the inelastic processes to the spin torque. As model systems we use the well defined tunneling junction of an STM consisting of a paramagnetic tip separated from a ferromagnetic electrode by a vacuum barrier. Three different single-crystal ferromagnets were used as magnetic electrodes: bcc Fe(100) and fcc Co on Cu(111) and on Cu(100). The paramagnetic tungsten tip ensures that the selection rules for magnon excitation stay simple and the experiments can be interpreted in a straightforward way. Nevertheless, the results are of general nature and hold also for the case of two magnetic electrodes, which is the configuration of interest for applications.

II. SELECTION RULES

First, we discuss which hot electrons can inelastically create magnons using quantum-mechanical selection rules for magnon creation. Without restriction of generality, we focus the discussion on one ferromagnetic electrode that is exposed

to a tunneling current from a nonmagnetic second electrode. Further, we assume that the spin-orbit interaction in the ferromagnet is weak such that the total spin is a conserved quantity. Finally, we assume that the magnetization of the ferromagnet is mainly caused by the spin moments of the electrons in the Fermi sea of the ferromagnet, which is a reasonable approximation for itinerant ferromagnets studied here.

When a positive sample bias U is applied to the ferromagnetic electrode, electrons tunnel into the ferromagnet resulting in hot electrons above the Fermi level E_F [cf. Fig. 1(a)]. The hot electrons thermalize in the electrode by scattering with lattice defects, phonons, or other electrons. If these processes do not change the spin of the hot electron, no angular momentum is transferred between the current and the magnetization and no inelastic STT is exerted. If, however, a hot electron of minority character undergoes a spin-flip scattering event with one of the electrons of the Fermi sea, angular momentum is transferred between the current and the magnetization. Conservation of total spin results in an increase of
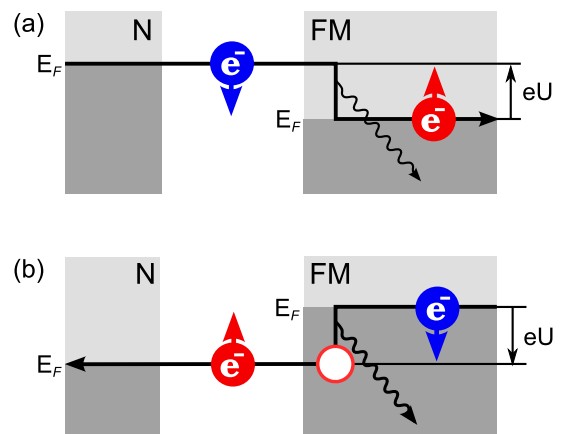

FIG. 1. (Color online) Magnon creation mechanism for tunneling (a) into and (b) out of a ferromagnetic electrode (right). The second electrode (left) is nonmagnetic. Magnons are created by minority electrons (blue, pointing down) tunneling into the ferromagnet and by majority electrons (red, pointing up) tunneling out of the ferromagnet.

$1\hbar$ in the spin of the current and a decrease of $1\hbar$ in the Fermi sea of the magnet. This process is equivalent to a creation of a magnon [cf. Fig. 1(a)]. As a result of the magnon creation, the individual spins of the ferromagnet are transversally displaced from their ground-state direction and precess around the local effective field identical to the case of a negative damping term due to the STT in the description of Slonczewski. The opposite process, a spin flip of a majority electron of the current into a minority electron, corresponds to the annihilation of a magnon or to an enhanced damping of the precession in the Slonczewski picture. In our study it is of importance that for positive U magnons can only be created by minority electrons tunneling into the ferromagnet. For negative U, electrons tunnel out of the ferromagnet thus creating holes. Again conservation of total spin results in the fact that only majority electrons that tunnel out of the ferromagnet can create magnons and can lead to a precession of the magnetization. They leave a majority hole, which can be filled by a minority electron of the electron sea by a spin flip. The filling of minority holes with majority electrons is equivalent to the annihilation of a magnon. In other words, for negative U magnons can only be created by majority electrons tunneling out of the ferromagnet [see Fig. 1(b)]. This transfer of momentum between the current and the magnetization is therefore equivalent to the inelastic STT.

III. MAGNON CREATION AND SPIN POLARIZATION

Second, we investigate experimentally how the magnon excitation scales with the spin polarization of the tunneling electrons and compare the experimental results to all electron *ab initio* calculations of the tunneling density of states. Inelastic tunneling spectroscopy (ITS) is the method of choice to study excitations created by tunneling electrons.[14] In elastic tunneling, the differential conductivity dI/dU is proportional to the density of states (DOS) of the electrodes.[15] In case the DOS does not vary rapidly at E_F, the $I(U)$ curve is a straight line, dI/dU is constant, and d^2I/dU^2 vanishes. When, however, the kinetic energy of the tunneling electrons is sufficient to create an inelastic excitation, an additional inelastic channel opens and the current is enhanced. As a consequence dI/dU shows a step at the excitation threshold energy and a peak in d^2I/dU^2 appears.[16] The relative step height in dI/dU is proportional to the excitation cross section. In case the excitation does not depend on the direction of the tunneling electrons, the dI/dU curve has a step for both polarities, and the d^2I/dU^2 has two peaks with opposite signs.[16]

The ITS experiments were performed in a home-built STM at 4.2 K in ultrahigh vacuum ($p < 4 \times 10^{-11}$ mbar). As has been shown previously, ITS using STM is well suited to detect spin-flip scattering as well as magnon excitation.[17–19] The STM experiments were performed on atomically clean samples with equally clean tips. The d^2I/dU^2 signal was measured with a lock-in amplifier detecting the second harmonics of a 2–3 mV, 2.6 kHz modulation. Fe(100), Cu(100), Cu(111), and the STM tip were cleaned by 1.5 keV Ar$^+$ sputtering and annealing. Co was deposited on the Cu sub-
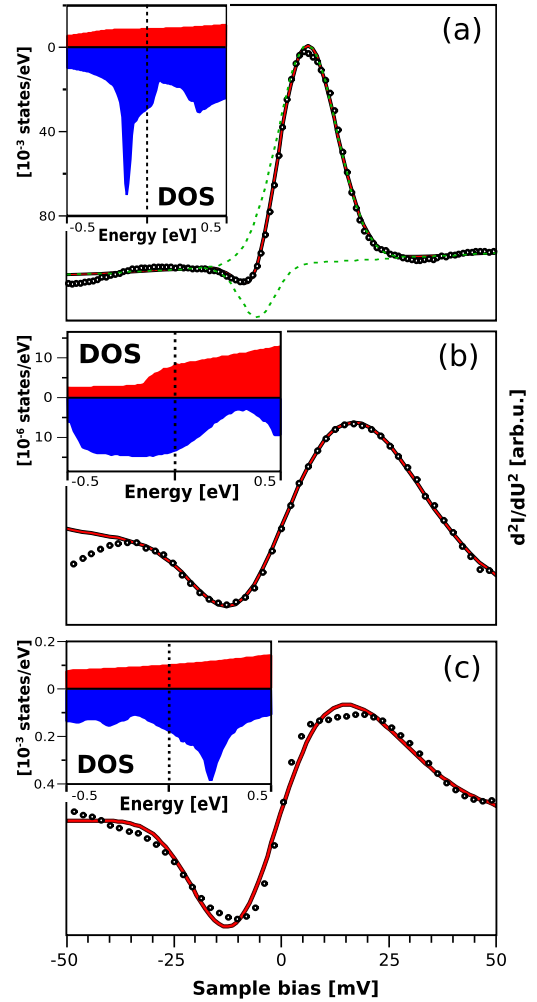

FIG. 2. (Color online) Inelastic tunneling (open circles) in (a) Fe(100), (b) 3 ML Co/Cu(111), and (c) 2 ML Co/Cu(100): double Gaussian fits of the two low energy excitation peaks are indicated as solid red lines. Insets: calculated majority (upper, red) and minority (lower, blue) DOS in states/eV at 4 Å above the surface. In (a) the two fitted Gaussians are indicated as green dashed lines.

strates by electron-beam evaporation from pure (99.99%) material. Scalar-relativistic density-functional theory calculations were used to determine the self-consistent electronic structure of Fe(100), as well as Co films on Cu(100) and on Cu(111). The local-spin density approximation (LSDA) to the exchange-correlation functional[20] was applied and the Korringa-Kohn-Rostoker multiple-scattering theory method[21,22] specially designed for semi-infinite systems was used. The DOS in the STM geometry was calculated within the Tersoff-Hamann approach[15] at a tip height of about 4 Å above the surface layer reflecting the STM experiment. The crystal structures including surface relaxation were adopted from experiments.[23–26]

We start with the investigation of bulk Fe(100). The calculated DOS shows the surface state of minority character near 300 meV (Ref. 27) as a peak and a volume band edge as peaks around −100 meV, while the majority density of states is smooth [cf. inset on Fig. 2(a)]. In the vicinity of the Fermi edge, the DOS for both spins are smooth. As a conse-

quence of the smooth DOS we expect a linear $I(U)$ curve. However, a small deviation from this linear behavior is observed around the Fermi energy E_F due to inelastic scattering, as has been reported before.[19] This deviation is best sensed in the second derivative of the tunneling current with respect to the bias voltage. Experimentally, a broad peak in the d^2I/dU^2 curve slightly above E_F [see Fig. 2(a)] and a weak dip below are observed. The peaks correspond to magnetic excitations, as has been proven recently with spin-polarized scanning tunneling spectroscopy.[19] Phonon and plasmon excitation could be ruled out, and in similar experiments on antiferromagnetic films the dispersion of the excitations could be verified to nicely agree with that of magnons.[28] The created magnons seen in the inelastic spectrum of Fig. 2(a) show energies up to 15 meV as will be discussed in detail later. The clear peak in the forward tunneling direction is accompanied by a weak negative peak for the opposite tunneling direction. This suggests a strong asymmetry for magnon creation between forward and backward tunneling. To evaluate this asymmetry, we fitted the experimental curve in the energy range of the two peaks close to E_F with a superposition of two Gaussians (a positive above and a negative below E_F) on a linear background, reflecting the creation of magnons in the forward and backward tunneling directions. The peak positions of the two Gaussians were chosen symmetrical with respect to E_F, while the peak areas were free to vary. The asymmetry α is defined as the difference of the areas of the Gaussians for negative and positive bias divided by their sum. The fit gives an asymmetry of -0.61 ± 0.04.[29]

In case the observed inelastic excitations are indeed magnons and as such contribute to the inelastic STT, they should obey the selection rules discussed above. The experimental asymmetry should then be identical to the spin polarization of the tunneling current. This simple relation is due to the fact that the number of created magnons in both tunneling directions scales with the number of tunneling electrons of the relevant spin character. Since in our experiments the STM tip is paramagnetic, the spin polarization of the current is given by the spin polarization of the DOS of the magnetic electrode within the Tersoff-Hamann model.[30] As shown in Fig. 2(a), the DOS near E_F displays a strong asymmetry. The low DOS in the majority channel (0.009 states/eV) with respect to the minority channel (0.03 states/eV) explains the small inelastic magnon peak in backward tunneling direction with respect to forward tunneling. The *ab initio* calculations give a spin polarization of the DOS at the Fermi level of -0.54 in good agreement with the asymmetry found for magnon creation.

We note here that for metal surfaces, p- and d-electron states are stronger localized and fall off more rapidly into the vacuum than s electrons. As a consequence the main contribution to the tunneling current in STM experiments with vacuum barriers comes from the s-electron states which then determine the spin polarization of the tunneling current.[31] For itinerant ferromagnets this can be negative or positive depending on the surface orientation. This is in contrast to planar tunnel junctions with oxide barriers, where other effects such as the hybridization of the metal and insulator orbitals at the interface determine the sign of the spin polarization.[32]
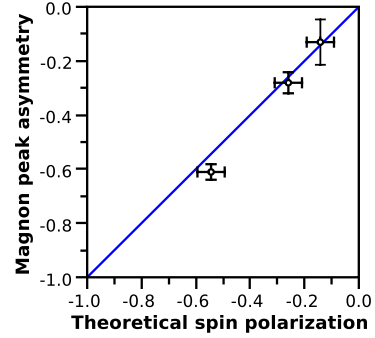

FIG. 3. (Color online) Comparison between theoretical spin polarization and experiment asymmetries. Calculation error was taken to be 5%. The straight line corresponds to $p_{exp}=p_{theor}$.

To show that these findings are not a coincidence but a general effect, we carried out identical experimental studies on thin fcc Co films on Cu(100) and on Cu(111). The obtained d^2I/dU^2 spectrum for tunneling between W and 3 monolayers (ML) of Co on Cu(111) is presented in Fig. 2(b) and a spectrum of 2 ML Co/Cu(100) in Fig. 2(c). Similar to bulk Fe, the inelastic tunneling spectra reveal the creation of magnons with energies up to 30 meV. The higher energies in Co with respect to Fe are most likely related to the higher exchange stiffness in Co, as will be discussed below. Similar Gaussian fits to the two excitation peaks near E_F result in an asymmetry of -0.28 ± 0.05 for Co/Cu(111) and of -0.13 ± 0.08 for Co/Cu(100). The calculated DOS [inset of Fig. 2(b) and 2(c)] shows a spin polarization of -0.26 and of -0.14 for Co on Cu(111) and on Cu(100), respectively.

To sum up these results, a comparison of experimental asymmetries and theoretical spin polarizations is shown in Fig. 3. The results for the three systems are in good agreement to theory thus illustrating the strict relation between the spin polarization of the tunneling current and the asymmetry of the magnon creation in forward and backward tunneling directions. Since a magnon creation is equivalent to a transfer of angular momentum, this result shows a linear dependence of the inelastic STT on the spin polarization of the tunneling current. This dependence was often assumed[10] and is now experimentally proven. We note that the observed inelastic spectra fully reflect the symmetry behavior of the STT, in which a reversal of the polarization or a reversal of the current direction leads to a reversal of the torque.[1]

IV. SIZE OF THE INELASTIC STT

Third, we investigate the absolute size of the inelastic STT. For this we focus on the ITS experiments performed on Fe. Figure 4 shows the dI/dU spectrum. As discussed above, the excitation of magnons results in a step in the dI/dU spectrum visible around E_F. The height of the step relative to the dI/dU signal is proportional to the fraction of the electrons that undergo inelastic scattering. From this fraction and the fact that these electrons transfer each a quantized moment of $1\hbar$ to the ferromagnet, we evaluated the size of the torque $\tau(U)$ of the inelastic STT in units of $\hbar$ per electron. Note, that in this case only one electrode is ferromagnetic
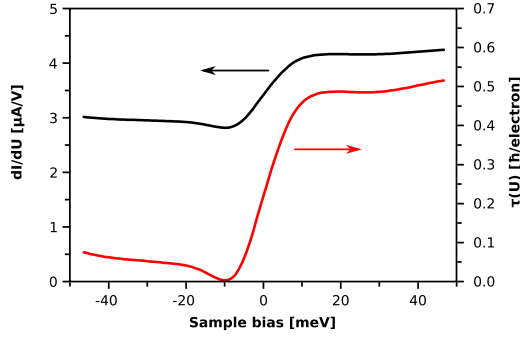
FIG. 4. (Color online) dI/dU spectrum of Fe(001) obtained with a W tip (black) as well as spin torque τ (red) as function of bias voltage.

FIG. 5. (Color online) Measured excitation spectrum on Fe(100) (red) in comparison to theoretical model (black).

and as such, the torque is no function of the magnetization direction but is determined by the change in angular momentum due to spin scattering. To describe an arbitrary direction of the spin polarization of the tunneling current in experiments with magnetic tunneling junctions, a linear combination of minority and majority electrons can be used, i.e., it is sufficient to investigate the scattering of minority and majority electrons to fully describe the STT.

First of all, one notices that in forward tunneling direction, inelastic spin scattering is very efficient. Up to 48% of all electrons are inelastically scattered at bias voltages above ≈ 10 mV. Taking into account the determined spin polarization between -0.54 and -0.61, this result means that $\approx 60\%$ of the tunneling minority electrons scatter inelastically via creation of magnons. At lower bias, the scattering process becomes less efficient until it finally vanishes at energies below the magnon gap. This clearly shows that the inelastic STT cannot be neglected in the full description of the STT in tunneling junctions. In fact, it might even be the dominant term at bias voltages above a few tens of millivolts. Further we have shown in a recent paper, that about 4% of the tunneling electrons scatter inelastically per atomic Co layer at bias voltages higher than 30 mV.[19] This implies that the inelastic STT is a surface effect which acts in the first ≈ 5 nm of the ferromagnet similar to the elastic STT.

V. QUANTUM MECHANICS OF THE SCATTERING MECHANISM

Fourth, we focus on the energy of the excited magnons and the primary spin scattering mechanism. The energy distribution of excited magnons can be obtained directly from the inelastic tunneling spectra. All spectra shown exhibit broad inelastic peaks at bias voltages around 10 mV. The excited magnons are therefore hyperthermal in our case, i.e., they raise the spin temperature of the ferromagnet above the experimental temperature of 4.2 K. We are, however, left with the question, why magnons of this particular energies are excited more efficiently than others. To answer this we focus on the spin scattering process of a hot electron, which is needed for magnon creation. To flip the spin, a potential $J(r)$ is required that couples the spin of the hot electron to the spins of the ferromagnet. As the hot electron in our investi-
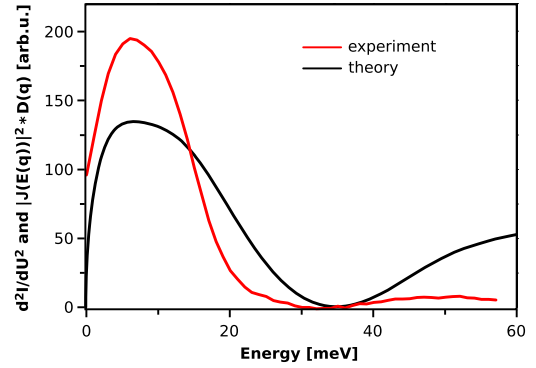
gations is relatively close to E_F, we can approximate the potential with the Ruderman-Kittel-Kasuya-Yosida (RKKY)-like exchange interaction that couples electron spins near E_F.[33] To first order the traveling hot electron will scatter with the spins of the magnetization via this potential. Note that due to the itinerant nature of the ferromagnet, the exchange is nonlocal, i.e., is not a point interaction but is carried by the delocalized electrons. The scattering cross section σ of the hot electron can be calculated within the Born approximation from the interaction potential $J(r)$. We only consider spin scattering and neglect scattering that changes the orbital momenta of the electrons. In this case, σ is given by the square of the Fourier transform of the interaction potential $J(q)$. Here, q is the momentum transfer, i.e., the magnon momentum. To obtain $\sigma(E)$, we express E as function of q, i.e., we use the dispersion relation for magnons and integrate over all magnons with the same energy. Therefore $\sigma(E) = |J[q(E)]|^2 * D(E)$, where $D(E)$ is the magnon density of states. We used a classical Heisenberg Hamiltonian and the magnetic force theorem[33,34] to calculate $J(q)$ and the spin-wave stiffness *ab initio*. The latter was estimated as 300 meV Å^2 for Fe. The resulting $\sigma(E)$ is plotted in Fig. 5 together with a background corrected[35] inelastic tunneling spectrum for bulk Fe.

Even though our model uses several approximations the agreement between experiment and theory is surprisingly good. All the main features are found in both: the maximum at low energies as well as the minimum around 35 meV and the increase in the cross section at even higher energies. The maximum is caused by the oscillatory nature of the RKKY-like exchange interaction in real space which translates to a peak in reciprocal space. The quantitative agreement at higher energies is not perfect, which is most likely due to the large scattering probabilities causing the cross section to saturate at high energies. Note that the maxima in d^2I/dU^2 for Fe are located at lower bias voltages than those of Co. This is most likely related to the much higher spin-wave stiffness in Co in comparison to Fe (≈ 600 meV Å^2 compared to ≈ 300 meV Å^2).[33] In the calculation of the magnon dispersion, the magnetic anisotropy of Fe was neglected. The modification of the dispersion due to anisotropy is, however, only of the order of few μeV and can thus be neglected in our study.

This spin-flip scattering mechanism of hot electrons might also be of relevance for the large difference in the mean-free

path for minority and majority electrons found for ballistic election emission microscopy[36] and for the fast thermalization of the spin temperature in electronic excitation of ferromagnets by ultrashort optical pumping.[37] In the latter, the inelastic mean-free path of ≈ 5 nm found for Co (Ref. 19) converts to a time constant of thermalization of ≈ 50 fs when taking an average Fermi velocity of 10^5 m/s for Co.

VI. CONCLUSION

In summary, we have shown that inelastic scattering is an important contribution to the STT, that its underlying mechanism is the spin scattering of electrons via the RKKY-like exchange interaction with electrons of the ferromagnet and that the excited magnons are of a relatively high energy up to a few tens of meV. The energy distribution of the excited magnons in the STT is of fundamental interest as it is intimately linked to the evolution of the magnetization vector field during current induced switching when going beyond the macrospin approximation. When modeling the spin torque effect in nanostructures in the macrospin approximation, these high-energy magnons are equivalent to a reduction in the effective magnetization of the nanostructure as, e.g., observed in recent spin torque experiments.[10] Further, we demonstrated that the asymmetry of the magnon excitation in forward and backward tunneling directions scales with the spin polarization of the tunneling current.

[1] J. C. Slonczewski, Phys. Rev. B **39**, 6995 (1989).

[2] L. Berger, Phys. Rev. B **54**, 9353 (1996).

[3] E. B. Myers, D. C. Ralph, J. A. Katine, R. N. Louie, and R. A. Buhrman, Science **285**, 867 (1999).

[4] M. Tsoi, A. G. M. Jansen, J. Bass, W.-C. Chiang, V. Tsoi, and P. Wyder, Nature (London) **406**, 46 (2000).

[5] Y. Huai, F. Albert, P. Nguyen, M. Pakala, and T. Valet, Appl. Phys. Lett. **84**, 3118 (2004).

[6] G. D. Fuchs, N. C. Emley, I. N. Krivorotov, P. M. Braganca, E. M. Ryan, S. I. Kiselev, J. C. Sankey, D. C. Ralph, R. A. Buhrman, and J. A. Katine, Appl. Phys. Lett. **85**, 1205 (2004).

[7] D. Chiba, Y. Sato, T. Kita, F. Matsukura, and H. Ohno, Phys. Rev. Lett. **93**, 216602 (2004).

[8] G. D. Fuchs, I. N. Krivorotov, P. M. Braganca, N. C. Emley, A. G. F. Garcia, D. C. Ralph, and R. A. Buhrman, Appl. Phys. Lett. **86**, 152509 (2005).

[9] M. Elsen, O. Boulle, J.-M. George, H. Jaffrès, R. Mattana, V. Cros, A. Fert, A. Lemaitre, R. Giraud, and G. Faini, Phys. Rev. B **73**, 035303 (2006).

[10] J. C. Sankey, Y.-T. Cui, J. Z. Sun, J. C. Slonczewski, R. A. Buhrman, and D. C. Ralph, Nat. Phys. **4**, 67 (2008).

[11] H. Kubota, A. Fukushima, K. Yakushiji, T. Nagahama, S. Yuasa, K. Ando, H. Maehara, Y. Nagamine, K. Tsunekawa, D. D. Djayaprawira, N. Watanabe, and Y. Suzuki, Nat. Phys. **4**, 37 (2008).

[12] J. C. Slonczewski, Phys. Rev. B **71**, 024411 (2005).

[13] P. M. Levy and A. Fert, Phys. Rev. Lett. **97**, 097205 (2006).

[14] B. C. Stipe, M. A. Razaei, and W. Ho, Science **280**, 1732 (1998).

[15] J. Tersoff and D. R. Hamann, Phys. Rev. Lett. **50**, 1998 (1983).

[16] E. L. Wolf, *Principles of Electron Tunneling Spectroscopy* (Oxford University Press, New York, 1985).

[17] A. J. Heinrich, J. A. Gupta, C. P. Lutz, and D. M. Eigler, Science **306**, 466 (2004).

[18] C. F. Hirjibehedin, C. P. Lutz, and A. J. Heinrich, Science **312**, 1021 (2006).

[19] T. Balashov, A. F. Takács, W. Wulfhekel, and J. Kirschner, Phys. Rev. Lett. **97**, 187201 (2006).

[20] J. P. Perdew and Y. Wang, Phys. Rev. B **45**, 13244 (1992).

[21] J. Korringa, Physica (Amsterdam) **13**, 392 (1947).

[22] W. Kohn and N. Rostoker, Phys. Rev. **94**, 1111 (1954).

[23] K. O. Legg, F. Jona, D. W. Jepsen, and P. M. Marcus, J. Phys. C **10**, 937 (1977).

[24] K. Heinz, S. Müller, and L. Hammer, J. Phys.: Condens. Matter **11**, 9437 (1999).

[25] A. Clarke, G. Jennings, R. F. Willis, P. J. Rous, and J. B. Pendry, Surf. Sci. **187**, 327 (1987).

[26] H. Li and B. P. Tonner, Surf. Sci. **237**, 141 (1990).

[27] J. A. Stroscio, D. T. Pierce, A. Davies, R. J. Celotta, and M. Weinert, Phys. Rev. Lett. **75**, 2960 (1995).

[28] C. L. Gao, A. Ernst, G. Fischer, W. Hergert, P. Bruno, W. Wulfhekel, and J. Kirschner, Phys. Rev. Lett. **101**, 167201 (2008).

[29] Note that due to the small intensity of the Gaussian at negative bias, the minimum of the combined Gaussians in the fit appears at lower energies.

[30] S. Heinze, P. Kurz, D. Wortmann, G. Bihlmayer, and S. Blügel, Appl. Phys. A: Mater. Sci. Process. **75**, 25 (2002).

[31] S. F. Alvarado, Phys. Rev. Lett. **75**, 513 (1995).

[32] J. M. de Teresa, A. Barthélémy, A. Fert, J. P. Contour, F. Montaigne, and P. Seneor, Science **286**, 507 (1999).

[33] M. Pajda, J. Kudrnovsky, I. Turek, V. Drchal, and P. Bruno, Phys. Rev. B **64**, 174402 (2001).

[34] A. I. Liechtenstein, M. I. Katsnelson, V. P. Antropov, and V. A. Gubanov, J. Magn. Magn. Mater. **67**, 65 (1987).

[35] A linear background in accordance with the fit of Fig. 2(a) was subtracted.

[36] W. H. Rippard and R. A. Buhrman, Phys. Rev. Lett. **84**, 971 (2000).

[37] L. Guidoni, E. Beaurepaire, and J.-Y. Bigot, Phys. Rev. Lett. **89**, 017401 (2002).